Energy 234 (2021) 121233

Contents lists available at ScienceDirect

Energy

journal homepage: www.elsevier.com/locate/energy

Remaining useful life prediction of lithium battery based on capacity regeneration point detection

Qiuhui Ma [a], Ying Zheng [a, *], Weidong Yang [a], Yong Zhang [b], Hong Zhang [a]

[a] *The Key Laboratory of Image Information Processing and Intelligent Control, School of Artificial Intelligence and Automation, Huazhong University of Science and Technology, Wuhan, 430074, China*
[b] *School of Information Science and Engineering, Wuhan University of Science and Technology, Wuhan, 430081, China*

ARTICLE INFO

Article history:
Received 31 July 2020
Received in revised form
8 June 2021
Accepted 11 June 2021
Available online 17 June 2021

Keywords:
Capacity regeneration
RUL
Lithium battery
Particle filter
Mann-Whitney *U* test
Autoregressive model

ABSTRACT

Lithium batteries have been widely used in various electronic devices, and the accurate prediction of its remaining useful life (RUL) can prevent the occurrence of sudden equipment failure. Battery capacity is a commonly used indicator to represent the health status of lithium batteries. However, the capacity regeneration is usually unavoidable due to the impact of battery "rest time" between two cycles, which leads to inaccurate prediction of the RUL. To solve this problem, this paper combines the particle filter (PF) and Mann-Whitney *U* test (PF-U) to detect the capacity regeneration point (CRP). In this light, the autoregressive (AR) model and PF algorithm are adopted for RUL prediction. The predicted capacity through AR model is used to update the degradation model parameters of PF algorithm, and the validation of our approach is verified through the lithium battery dataset of NASA. In comparison, our proposed method exhibits the highest precision and provides a platform to detect the points with capacity regeneration, and further reduce the RUL prediction error.

1. Introduction

Due to high energy density, wide operating temperature range, and quick charging/discharging speed, lithium batteries have been widely used for power supply in transportation, electric storage, mobile communication, etc [1]. Owing to its internal physical structure as well as external environmental conditions, the performance of lithium battery will decline. The degradation of lithium battery will reduce system reliability, and even lead to catastrophic accidents. Therefore, it is crucial to describe and predict the degradation tendency of lithium battery accurately in battery management system [2,3]. It will provide effective information to assist the operator maintain and replace the battery in a timely manner, thus to extend the battery life and prevent security risks [4,5].

In recent years, the SOH estimation and RUL prediction are two vital research aspects in battery management system. SOH is an indicator reflecting the health state of battery in the short term, while RUL is a long-term indicator that shows the remaining cycle life before SOH drops to a predefined threshold [3]. Generally, there are mainly three type of RUL prediction models, i.e., the data-driven, physical-of-failure-based (PoF) model and hybrid empirical model [6].

The data-driven method does not need to consider the internal mechanism of the degradation procedure, and only needs to establish the relationship between degraded data and health state through some statistical analysis or machine learning methods [7]. Liu et al. [8] introduced the relevance vector machine (RVM) for RUL prediction and the probability distribution function representing the uncertainty of the predicted result. Yang et al. [9] utilized the SVR to estimate the SOH of lithium battery. Generally, the extracted features, such as the time interval of equal charging voltage difference, charging capacity [10], energy of signal and fluctuation of signal [11], are used as the inputs to SVR, and SOH is used as outputs to predict RUL finally. Pan et al. [12] proposed an extreme learning machine to capture the underlying correlation between the extracted health indicators and capacity degradation to improve the speed and accuracy of machine learning for online estimation. Bian et al. [13] trained a stacked bidirectional long short-term memory neural network model for SOH estimation of lithium battery. In contrast to unidirectional recursive neural networks (RNNs), they employ a bidirectional structure to capture sequential temporal information including voltage, current, and

* Corresponding author.
E-mail address: zyhidy@mail.hust.edu.cn (Y. Zheng).

https://doi.org/10.1016/j.energy.2021.121233
0360-5442/

Nomenclature

Q_k	Actual capacity at kth cycle (Ah)
u_k	The process noise
v_k	The observation noise
k	The discharging cycle number
ϕ	Autoregression coefficient
$\hat{\phi}$	The estimated Autoregression coefficient
x_k	The state variable
$\hat{Q}_k$	The prior estimated capacity (Ah)
$\tilde{Q}_k$	The updated capacity (Ah)
$U(k)$	The testing statistics
U_z	The known critical value
μ	The mean value
σ	The standard deviation
$q(x)$	The importance sampling density function
$\hat{Y}_k$	The prior estimated capacity with M particles (Ah)
$\tilde{Y}_k$	The updated capacity with M particles (Ah)
Q_{AR}	The estimated capacity based on AR algorithm (Ah)
Q_{PF}	The estimated capacity based on PF algorithm (Ah)
$\hat{Q}_{AR}$	The predicted capacity based on AR algorithm (Ah)
$\hat{Q}_{PF}$	The predicted capacity based on PF algorithm (Ah)
M	The number of particles
TH	Failure threshold
Acc	Accuracy
a_k	A white noise sequence
$\delta(\cdot)$	Dirac function
ST	Starting point
Pre	Precision
RR	Recall rate
$RMSE$	Root-mean-square error
R^2	R square
seq	A random sequence
err	Training errors
K_f	The failure cycle
TP	True positive
TN	True negative
FP	False positive
FN	False negative
RUL_r	The actual RUL
RUL_p	The predicted RUL
RUL_m	Mean of the RUL

temperature in both forward and backward directions, and summarized temporal dependencies from past and future contexts. However, the data-driven method is like a black box, it requires large amounts of data for training, and the prediction data should follow the similar distribution with the training data, otherwise data-driven method cannot guarantee the prediction accuracy.

The physical-of-failure-based (PoF) model utilizes the knowledge of failure mechanism to predict RUL of lithium battery. Some scholars established electrochemical models and equivalent circuit models, etc. to explore the degradation mechanism of batteries. For example, Safari et al. [14] developed a multimodal physics-based aging model that can be used both in cycling and storage condition. The model is based on the continuous, small-scale growth of a solid electrolyte interphase (SEI) layer on the surface of the anode active particles. Tian et al. [15] proposed an aging mode identification method based on open-circuit voltage matching analysis. The open-circuit voltage model of the full cell is established based on the state of charge matching relationship between the full cell and electrodes. Although excellent prediction accuracy can be achieved, mechanism modeling is a complicated and difficult task. Hence, the hybrid empirical model based on the prior knowledge of degradation process is widely used due to its simplicity and reliability in recent researches. A certain model will be proposed firstly to reflect the relationship between battery SOH and its inner or outer characteristics such as cycle number, discharge voltage, temperature, inner impedance, etc. Then the model parameters are estimated by such methods as Kalman filter (KF), particle filter (PF) and their variants [16–18]. Pan et al. [19] proposed a novel open-circuit voltage model based on cubic Hermite interpolation to update the state estimate. He [20] and Liu et al. [3] introduced an empirical exponential model to estimate the capacity fade data, the parameters of which were identified by particle filtering. Shen et al. [21] utilized nonlinear Wiener process to model the capacity degradation process, and estimated the model parameters online by unscented particle filter (UPF). In addition, other empirical models such as double exponential [22], linear [23] and polynomial models [24] are also used to establish the degradation process and obtain the accurate RUL prediction results for the lithium batteries.

The capacity of a lithium battery shows a degradation trend because of the side reactions that occur between the electrodes and electrolyte of the battery. Therefore, it is usually selected as a health indicator for battery degradation empirical model in the above-mentioned. However, there is a common phenomenon of so-called capacity regeneration (CR). That is, if the battery rests during charge/discharge profiles, the residual reaction products have a chance to dissipate, and the available capacity for the next cycle will be increased immediately [25].

The phenomenon of capacity regeneration obviously affects RUL prediction of the lithium batteries. In the past years, there are few researches on the effect of CR on RUL prediction. Further, most of literatures among them focused on how to remove the capacity regeneration point (CRP) from the degradation process, so that only the part of the decline curve can be obtained. Jin et al. [26] adopted an exponential model to remove the data of the CRPs. In some researches, these CRPs are recognized as noise, then filtering methods are utilized to smooth the curve. Removing the CRP directly will lose some information, but the existence of CRP makes the degradation curve of capacity more nonlinear and increase the difficulty of RUL prediction. To solve this problem, Pang et al. [25] used the multi-scale wavelet decomposition technology to separate the global degradation and local regeneration of a battery capacity series, then constructed the RUL prediction framework based on nonlinear auto regression neural network model to combine two parts of the prediction results. Besides, capacity regeneration phenomenon is related to the rest time which is determined by practical demands. To accurately predict the regeneration phenomenon, Qin et al. [27] proposed a similar rest time-based prognostic framework. They adopted the particle swarm optimization algorithm to determine the threshold of historical battery, and used a linear model to predict regeneration amplitude and regeneration point. Finally, the amplitude, regeneration point and threshold were integrated to estimate the final SOH. Deng et al. [28] proposed a condition-based empirical model which is consist of global degradation process and several local degradation processes affected by regeneration phenomena. They detected the regeneration phenomenon occurrence by a step function according to the rest time between two adjacent charge/discharge cycles. Since the rest time is random, it is difficult to explore the relationship between the rest time and the amplitude of the regeneration. Therefore, in some researches, the capacity regeneration is detected as an anomaly point which is not expected to occur. Orchard et al. [29] compared some approaches to detect the regeneration phenomenon, such as entropy-based approach, Kullback-Leibler divergence-based approach, and so on. Wang et al. [30] considered the locations of CRP as an unobserved latent random variable, and introduced the expectation-maximization algorithm to iteratively calculate probabilities of such variables so as to monitor capacity regeneration phenomenon.

Motivated by above-mentioned works, in this paper, the capacity regeneration phenomenon is considered in the degradation process of lithium batteries, and a novel scheme of the RUL prediction with automatic CRP detection is proposed thereby. Firstly, the CRP detection is carried out based on PF and Mann Whitney *U* test. Then, a hybrid model combining PF and AR model is proposed to predict the RUL of lithium batteries. The predicted value of AR model is taken as the actual value to update the parameters of the PF model to achieve accurate RUL prediction. The final result is obtained by combining the RUL prediction with the deviation between the substitution point and CRP. The main contribution of this paper is listed as follows: 1) A new framework combines the CRP detection and RUL prediction is set up to solve the prediction problem caused by CRP. 2) the PF-U based capacity regeneration detection method is proposed, which can accurately detect the CRP of different batteries. 3) the hybrid PF-AR model based RUL prediction is proposed, which will reduce the prediction error.

The rest of the paper is organized as follows: Section 2 formulate the problem by introducing the influence of capacity regeneration phenomenon on RUL prediction error. Section 3 describes the proposed CRP detection and RUL prediction methodology. In Section 4, experimental research on lithium battery's dataset from NASA confirms the effectiveness of the proposed algorithm. Finally, conclusions are given in Section 5.

2. Problem formulation

For the degradation process of lithium battery, since the double exponential model has superior predictive performance compared with other models such as polynomial model [24], it is adopted in this paper as Eq. (1) to establish the degradation model:

$$Q_k = a_k \cdot exp(b_k \cdot k) + c_k \cdot exp(d_k \cdot k) \tag{1}$$

where k represents the discharging cycle number, and Q_k denotes the capacity of the kth cycle; a_k, b_k, c_k, d_k and represents the model parameters that need to be determined. Set $x_k = [a_k, b_k, c_k, d_k]$, and rewrite Eq. (1) as follows by considering the noise in the degradation process:

$$\begin{aligned} x_k &= x_{k-1} + u_k \\ Q_k &= a_k \cdot exp(b_k \cdot k) + c_k \cdot exp(d_k \cdot k) + v_k \end{aligned} \tag{2}$$

where $u_k \sim N(0, W_0)$ is the process noise and $v_k \sim N(0, R_0)$ is the observation noise.

The degradation process of lithium batteries involves complex electrochemical reaction, which lead to the nonlinear characteristics. Specifically, when the lithium battery is at the 'rest' state, its capacity will be regenerated and increase rapidly to a certain extent. If the RUL is predicted at this time, the prediction error will rise greatly. The more capacity is regenerated, the greater RUL prediction error there will be.

Take B0006 battery from NASA lithium battery data set [31] as an example. As shown in Fig. 1, the actual capacity in blue has a large regeneration at the 90th cycle, which is 0.1519Ah higher than the previous cycle. Without loss of generality, a widely-used Particle Filter (PF) algorithm is adopted for RUL prediction in this example. When the starting time (ST) of the prediction is 90th cycle, the predicted end of life (EOL) by PF algorithm is 193rd cycle (in pink), and the real EOL is 157th cycle so that the predicted error is 36 cycles. While when the starting time is 92nd cycle, the prediction error is reduced rapidly to 9 cycles (in green); and if ST changes to be 95th cycle, the error is only 3 cycles (in black).

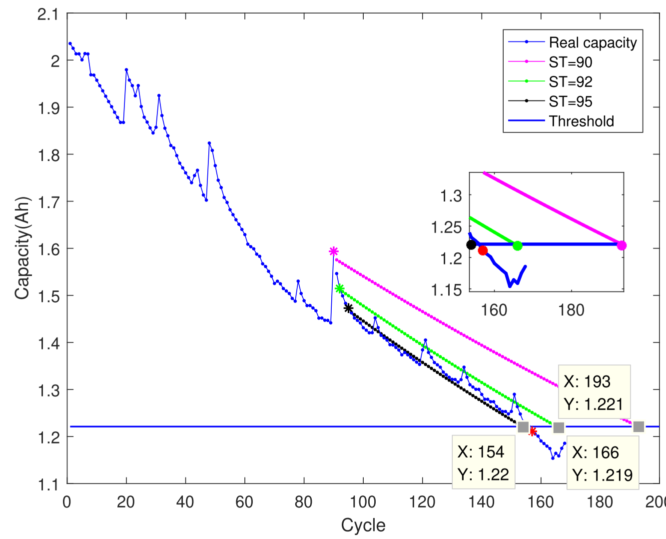

Fig. 1. RUL prediction from the different points.

Therefore, the capacity regeneration has a relatively significant impact on the actual prediction, and the point with a large capacity rise should be avoided to be used as the starting time to predict RUL. In this paper, the capacity regeneration will be discussed and considered, and a capacity regeneration point (CRP) detection algorithm is proposed. Based on the result of CRP detection, the combined particle filter and auto regression model is utilized to predict the RUL of lithium batteries.

3. Methodology

The objective of this work is to solve the problem of inaccurate RUL prediction that is due to the existence of large capacity regeneration. Fig. 2 shows the flow chart of the methodology, which is divided into capacity degradation modeling, CRP detection and RUL prediction. In section 3.1, the estimation model based on particle-filter algorithm is explained, and section 3.2 describes the CRP detection by combining particle-filter and Man-Whitney *U* test. Section 3.3 introduces a hybrid RUL prediction method based on PF-AR model. Finally in section 3.4, the procedure of the proposed method is presented in detail.

3.1. Particle filter-based estimation method

Compared with the Kalman filter (KF) and Extend Kalman filter (EKF) which are based on Gaussian noise assumption and local linearized model, PF is a more general solution for parameter identification of a nonlinear and non-Gaussian model.

In this paper, PF is used to estimate the parameters of the degradation model (2). The degradation model can be described by the state space model as follows:

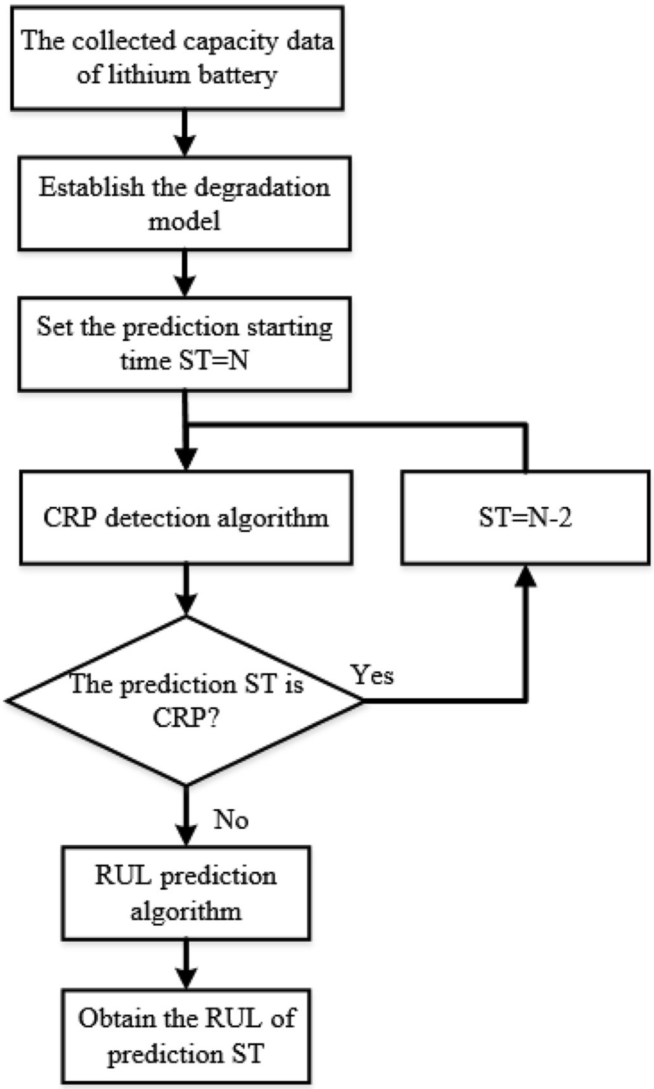

Fig. 2. The flowchart of the proposed method.

$$\begin{aligned} x_k &= f(x_{k-1}) + u_k \\ Q_k &= h(x_k) + v_k \end{aligned} \tag{3}$$

where $f(x_k) = x_k$ and $h(x_k) = h([a_k, b_k, c_k, d_k]) = a_k \cdot exp(b_k \cdot k) + c_k \cdot exp(d_k \cdot k)$ are the state transfer equation and the observation equation respectively. Based on Bayesian filter and Monte Carlo algorithm, the posterior probability density function (PDF) of the state is obtained through the state update and the measure update.

Assume the initial PDF of the state is $p(x_0|Q_0) = p(x_0)$, where x_0 is the initial value of the state variable, the one-step prediction of the state is:

$$p(x_k|Q_{1:k-1}) = \int p(x_k|x_{k-1})p(x_{k-1}|Q_{1:k-1})dx_{k-1} \tag{4}$$

where $Q_{1:k-1}$ represents the capacity from the 1st cycle to the $(k-1)^{th}$ cycle. Given the measured capacity Q_k, the posterior PDF after the state update is

$$p(x_k|Q_{1:k}) = \frac{p(Q_k|x_k)p(x_k|Q_{1:k-1})}{p(Q_k|Q_{1:k-1})} \tag{5}$$

where $p(Q_k|Q_{1:k-1}) = \int P(Q_k|x_k)p(x_k|Q_{1:k-1})dx_k$.

The integral operation in Eq. (5) is difficult to calculate, accordingly Monte Carlo method is used to generate a large amount of random particles and change the integral operation into the summation of particles. Specifically, the M particles, i.e., the M independent state variables with same distribution, are generated at the kth cycle and expressed as $x_k^{(i)}, i = 1,2,\ldots M$. Then the posterior PDF of the state can be approximated by the following Eq. (6):

$$p(x_k|Q_{1:k}) \approx \sum_{i=1}^{M} \omega_k^{(i)} \delta(x_k - x_k^{(i)}) \tag{6}$$

where $\omega_k^{(i)}$ is the normalized weight of sample $x_k^{(i)}$, and $\delta(\cdot)$ is a Dirac function. After resampling each particle, the corresponding weight is recursively updated as

$$\omega_k^{(i)} = \omega_{k-1}^{(i)} \frac{p(Q_k|x_k^{(i)})p(x_k^{(i)}|x_{k-1}^{(i)})}{q(x_k^{(i)}|x_{0:k-1}^{(i)}, Q_k)} \tag{7}$$

where $q(x_k)$ denotes the importance sampling density [32]. The choice of $q(x_k)$ is critical for the performance of the particle filter scheme. In this proposed method, $q(x_k|x_{k-1}) = p(x_k|x_{k-1})$.

The importance weight is gradually concentrated on a number of particles, so that the prediction result may deviate from the actual value. The random resampling algorithm is adopted in the proposed method to discard the sample points with small weight and select the sample points with large weight.

3.2. The PF-U based capacity regeneration point detection

By PF algorithm, the PDF of the prior state is calculated as $p(\hat{x}_k|x_{k-1})$. Then after being extracted from $p(\hat{x}_k|x_{k-1})$, the state value $\hat{x}_k$ substitutes x_k in the observation equation in Eq. (3) to obtain the prior estimate capacity $\hat{Q}_k$. Finally, the actual capacity Q_k is obtained and used to update $\hat{x}_k$, and the posterior PDF is computed as $p(\tilde{x}_k|Q_k)$, hence the updated capacity $\tilde{Q}_k$ can be obtained according to $\tilde{x}_k$.

The predicted capacity $\hat{Y}_k$ and the updated $\tilde{Y}_k$ with M particles can be expressed as $\hat{Y}_k = \left\{\hat{Q}_k^1, \hat{Q}_k^2, \ldots \hat{Q}_k^M\right\}$ and $\tilde{Y}_k = \left\{\tilde{Q}_k^1, \tilde{Q}_k^2, \ldots \tilde{Q}_k^M\right\}$. In general, the capacity decreases slowly except the capacity regeneration points. As a result, there will be a large difference in the distribution of $\hat{Y}_k$ and $\tilde{Y}_k$.

The Mann-Whitney U test was proposed by H.B. Mann and D.R. Whitney in 1947 [33]. It is a non-parametric test method to detect the difference of population distribution in two sample groups. In this section, Mann-Whitney U test is used to detect CRP by comparing the two groups $\hat{Y}_k$ and $\tilde{Y}_k$. After mixing the two groups and sorting them in ascending order, we calculate the sum of the corresponding order for the two groups as $S(\hat{Y}_k)$ and $S(\tilde{Y}_k)$ respectively. Hence, the corresponding Mann-Whitney U test statistics $U_1(k)$ and $U_2(k)$ are calculated as:

$$\begin{aligned} U_1(k) &= M^2 + \frac{M(M-1)}{2} - S(\hat{Y}_k) \\ U_2(k) &= M^2 + \frac{M(M-1)}{2} - S(\tilde{Y}_k) \end{aligned} \tag{8}$$

Select the smaller value between $U_1(k)$ and $U_2(k)$ as the final testing statistics $U(k)$. For $M < 10$, $U(k)$ is compared with the known critical value U_z to identify the difference between $\hat{Y}_k$ and $\tilde{Y}_k$. If $U(k) > U_z$, $\hat{Y}_k$ is quite different with $\tilde{Y}_k$, which means the capacity is regenerated at this point. For $M > 10$, the sampling distribution of $U(k)$ approximates to the normal distribution, and the corresponding mean and standard deviation are expressed as Eq. (9).

$$\begin{aligned} \mu_U &= \frac{M^2}{2} \\ \sigma_U &= \sqrt{\frac{M^2(2M+1)}{12}} \end{aligned} \tag{9}$$

Use $z(k) = \frac{U(k)-\mu_U}{\sigma_U}$ which obeys the standard normal distribution as testing statistics with a given level of confidence. The testing statistics are compared with its known control limit. Similarly, if the statistics exceeds the limit, the capacity regeneration exists at that cycle.

3.3. The RUL prediction algorithm based on PF-AR model

For the RUL prediction of lithium battery, the PF algorithm introduced in section 3.1 is widely used. However, it has the following two defects: (i) due to lack of actual capacity in the prediction stage, the parameters of degradation model Eq. (2) cannot be updated online; (ii) the PF algorithm relies excessively on the establishment of degradation model. Since autoregressive (AR) model has excellent long-term prediction performance, it is adopted to solve the above two problems of PF algorithm.

Since the capacity of lithium battery is a time series, its p-order AR model is expressed as follows:

$$Q_k = \phi_1 Q_{k-1} + \phi_2 Q_{k-2} + \cdots \phi_p Q_{k-p} + a_k \tag{10}$$

where $\phi \neq 0$ is autoregressive coefficient, and $a_k \sim N(0, \sigma_a^2)$ denotes a white noise sequence. It must be noted that ϕ, σ_a^2 and p need to be determined.

With the advantages of simple calculation and high accuracy, the least square estimation method is used to determine the parameters of AR model (10).

For the series $\{Q_k\}_{k=1,2\cdots N}$ with N training samples, when $k > p+1$, the estimated a_k can be expressed as

$$\hat{a}_k = Q_k - (\hat{\phi}_1 Q_{k-1} + \hat{\phi}_2 Q_{k-2} + \cdots \hat{\phi}_p Q_{k-p}) \tag{11}$$

where $\hat{a}_k$ is the residual, and $\hat{\phi}_1, \hat{\phi}_2, \cdots \hat{\phi}_p$ are the estimated autoregressive coefficients in Eq. (10). To extend Q_k to $[\,Q_{p+1} \quad Q_{p+2} \quad \cdots \quad Q_N\,]$, Eq. (10) is transformed as

$$Q = X\phi + a \tag{12}$$

where $Q = \begin{bmatrix} Q_{p+1} \\ Q_{p+2} \\ \cdots \\ Q_N \end{bmatrix}, X = \begin{bmatrix} Q_p & Q_{p-1} & \cdots & Q_1 \\ Q_{p+1} & Q_p & \cdots & Q_2 \\ \vdots & \vdots & \vdots & \vdots \\ Q_{N-1} & Q_{N-2} & \cdots & Q_{N-p} \end{bmatrix}, \phi = \begin{bmatrix} \phi_0 \\ \phi_1 \\ \vdots \\ \phi_p \end{bmatrix},$ $a = \begin{bmatrix} a_{p+1} \\ a_{p+2} \\ \vdots \\ a_N \end{bmatrix}.$

To minimize the sum of residual squares as Eq. (11), and the optimization function for AR model (12) is denoted as follow:

$$E(\phi) = min(Q - X\phi)^T(Q - X\phi) = min(Q^TQ - 2Q^TX\phi + \phi^TX^TX\phi) \tag{13}$$

Let $\frac{\partial(E(\phi))}{\partial\phi} = 0$, the least squares estimation of parameter ϕ and σ_a^2 can be obtained as

$$\hat{\phi} = (X^TX)^{-1}X^TQ \tag{14}$$

$$\hat{\sigma}^2 = \frac{1}{N-p}(Q - X\phi)^T(Q - X\phi) \tag{15}$$

Final prediction error (FPE) is adopted to determine the order p of AR model as follows:

$$FPE(p) = \left(1 + \frac{p}{N}\right)\left(1 - \frac{p}{N}\right)^{-1}\left(\hat{\gamma}_0 - \sum_{i=1}^{p}\phi_i\hat{\gamma}_i\right) \tag{16}$$

where $\hat{\gamma}_i$ are self-covariance of the samples with order i. The corresponding order with the minimum FPE is chosen for the AR model (12).

Given the starting time (ST) for RUL prediction as the N^{th} cycle, the measured actual capacity $Q = \{Q_1, Q_2, \cdots Q_N\}$ are collected in the training stage. The training model is established as an AR form (12) with the parameter identified by Eq.14–16, and the estimated capacity is obtained as $Y_{AR} = \{Q_{AR}(1), Q_{AR}(2), \cdots Q_{AR}(N)\}$. As for PF algorithm, the actual capacity $\{Q_1, Q_2, \cdots Q_N\}$ is used to update the parameters of the degradation model (2) by Eq. (6) and Eq. (7), and the estimated capacity is $Y_{PF} = \{Q_{PF}(1), Q_{PF}(2), \cdots Q_{PF}(N)\}$.

In the prediction stage, there is no actual capacity to update the parameters of the degradation model (2) with PF algorithm. The hybrid RUL prediction model is constructed by combining AR model (12) and PF algorithm. Firstly, the training errors between two models are computed as Eq. (17):

$$err(k) = Q_{PF}(k) - Q_{AR}(k) \tag{17}$$

where $k = 1, 2 \cdots N$.

Denote $Err = \{err(1), err(2), \cdots err(N)\}$, then a random sequence $seq(i) \sim N(mean(Err), var(Err))$ is generated. Thus, the 'actual' capacity $\hat{Q}_s(K)$ with $K = N+1, N+2, \cdots$ can be obtained as the sum of long-term predicted capacity $\hat{Q}_{AR}(K)$ and $seq(K)$ to update the parameters of degradation model (2) by Eq. (18).

$$\hat{Q}_s(K) = \hat{Q}_{AR}(K) + seq(K) \tag{18}$$

Based on the degradation model (2), the final predicted capacity is denoted as $\hat{Q}_o(K)$. Compare the $\hat{Q}_o(K)$ and capacity failure threshold, and regard the first point with the capacity below the threshold, i.e., $\hat{Q}_o(K_f)$, to be the beginning failure point. Accordingly, the time difference between the failure time and the starting time,i.e.,$K_f - ST$, is the RUL prediction at the N^{th} cycle.

3.4. The procedure of the proposed RUL prediction method

As described in Section 3.2, the CRP detection will help to improve the RUL prediction accuracy. The detected CRP is replaced by the points ahead of itself to get the final RUL prediction result. To sum up, the procedure of the proposed PF-AR model based RUL prediction algorithm with CRP detection is listed as follows:

Step 1: Initialize the parameters of degradation model (2) W_0, R_0 and the state variable x_0, set the starting time $ST = N$, obtain the actual capacity Q_k $(k = 1, 2\cdots N)$ as training data.

Step 2: According to the PF-U algorithm introduced in Section 3.2, the CRP are detected at starting time N. Replace $ST = N$ with $ST = N - 2$, the measured capacity Q_k $(k = 1, 2\cdots N - 2)$ are regarded as the corresponding training data.

Step 3: Obtain Q_{PF} and Q_{AR} with the training data by the method introduced in Section 3.3. Calculate Err by Eq. (17), and generate a random sequence $seq(i) \sim N(mean(Err), var(Err))$.

Step 4: Set the capacity failure threshold is TH, and $K = ST$.

Step 5: Calculate $\hat{Q}_s(K)$ by Eq. (18), use $\hat{Q}_s(K)$ as the 'actual' capacity to update the parameters of the degradation model (2) with PF algorithm, and obtain the predicted capacity $\hat{Q}_o(K)$ based on PF-AR model.

Step 6: Compare $\hat{Q}_o(K)$ and TH. If $\hat{Q}_o(K) > TH$, let $K = K + 1$ and repeat step 5 until $\hat{Q}_o(K) \le TH$.

Step 7: Calculate the RUL by $RUL = K - ST$.

4. Validation

In this section, the lithium-ion battery data provided by NASA are adopted. These batteries were tested on the Lithium battery accelerated life experiment platform. There are 9 groups of experiment data obtained under different operating conditions. Too high and too low room temperature will reduce the RUL of lithium battery, therefore battery B0005, B0006, B0007, and B0018 operating at room temperature (24 °C) are selected to verify the effectiveness of the proposed approach.

The lithium batteries were run through three different operational profiles (charging, discharging and impedance). During the charging procedure, the batteries are charged to 4.2 V at a constant current of 1.5A, and then charged at a constant voltage of 4.2 V until the current drops to 20 mA. During the discharging procedure, they are discharged to different voltage with the same current of 2A. Due to the different experimental conditions of four batteries, the failure threshold are chosen as 1.39Ah, 1.22Ah, 1.437Ah and 1.39Ah respectively. The capacity degradation procedures of these four batteries are shown in Fig. 3.

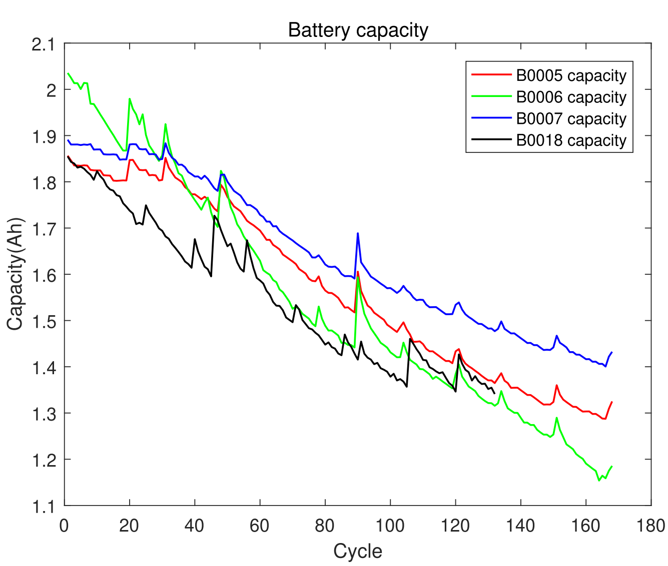

Fig. 3. The capacity degradation process of the four batteries.

In order to evaluate the performance of the CRP detection methods proposed in this paper, the accuracy Acc, precision Pre and recall rate RR are selected to assess CRP detection results. Besides, the traditional root-mean-square error $RMSE$ and R^2 coefficient are also used. These indicators are presented as follows:

$$Acc = \frac{TP + TN}{TP + TN + FP + FN} \tag{19}$$

$$Pre = \frac{TP}{TP + FP} \tag{20}$$

$$RR = \frac{TP}{TP + FN} \tag{21}$$

$$RMSE = \sqrt{\frac{1}{n}\sum_{k=1}^{n}\left(RUL_r(k) - RUL_p(k)\right)^2} \tag{22}$$

$$R^2 = 1 - \frac{\sum_{k=1}^{n}\left(RUL_r(k) - RUL_p(k)\right)^2}{\sum_{k=1}^{n}\left(RUL_r(k) - RUL_m(k)\right)^2} \tag{23}$$

where TP, TN, FP, FN represent the true positive, true negative, false positive and false negative respectively; RUL_r and RUL_p indicate the actual and the predicted RUL respectively, and RUL_m represent the mean of the RUL.

Specifically, the closer to 1 the indicator $Acc/Pre/RR$ is, the better the corresponding detection algorithm performs. While for the indicator $RMSE$ and R^2, being closer to 0 and 1 indicates higher capacity prediction accuracy respectively.

4.1. The PF-U based CRP detection

In this subsection, the effectiveness of the proposed CRP detection method is verified. As shown in Fig. 3, the capacity gradually decreases during the whole degradation process; while at some points, there exists capacity regeneration with the different range.

Take B0006 battery as an example, the battery capacity contains obvious increase in the 20th, 31st, 48th, 90th and 121th cycle and slight increase in 7th, 24th, 44th, 78th, 104th, 134th, 151th cycle. Set the number of particles $M = 200$, the confidence level as 0.01, and $x_0 = [1.97, -0.0027, -0.17, -0.069]$, $W_0 = 0.001$, $R_0 = 0.001$. When $N = 60$ cycles, the prior estimated $\hat{Y}_k = \left\{\hat{Q}_k^1, \hat{Q}_k^2, \cdots \hat{Q}_k^M\right\}$ and the posterior updated $\tilde{Y}_k = \left\{\tilde{Q}_k^1, \tilde{Q}_k^2, \cdots \tilde{Q}_k^M\right\}$ are calculated according to the method introduced in section 3.2, and then the M statistics are calculated as $\{z_1, z_2, \cdots z_M\}$. Fig. 4(a) shows the actual capacity curve; while Fig. 4(b) demonstrates the CRP detection result by the proposed method, and both the actual and detected CRPs are circled in red. It can be indicated that all the six CRPs are successfully detected. The detection accuracy is 96.67%, and the RR is 100%.

When $N = 80$ and 100 cycles, the detection results are shown in Figs. 5 and 6 respectively. It can be seen that the CRPs have been completely detected. In addition, according to Figs. 4–6, different training number N will not affect the CRP detection result by the proposed PF-U based method.

In order to show the applicability of the PF-U based detection method for different batteries, the verification test on B0005,

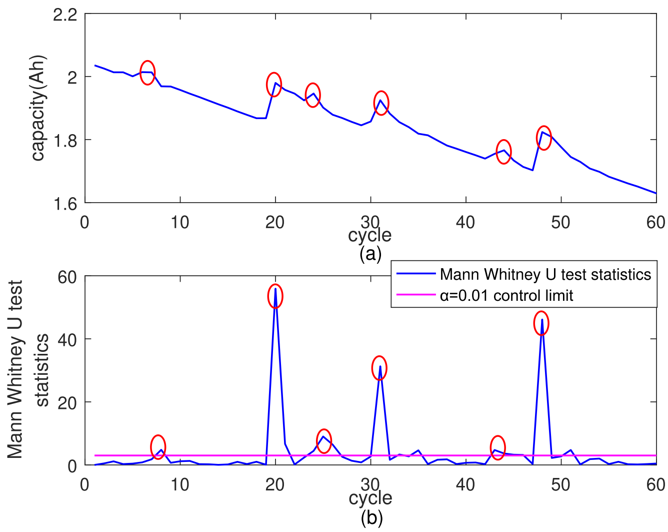

Fig. 4. The detection results of B0006 at N = 60 cycles. (a)The actual capacity regeneration points. (b) The detected capacity regeneration points.

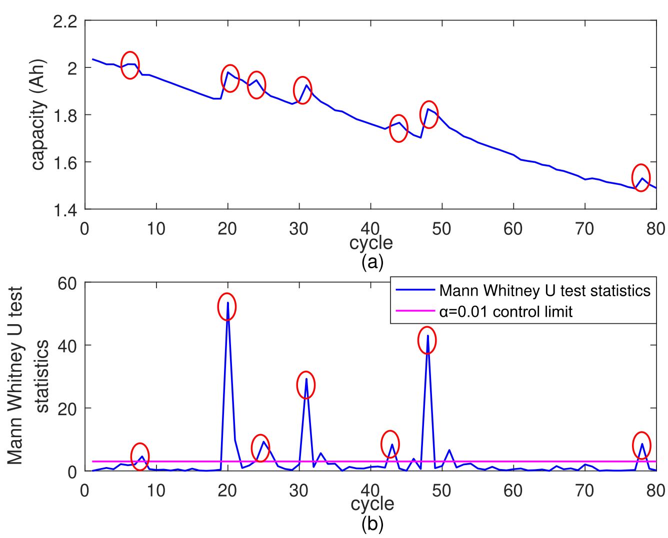

Fig. 5. The detection results of B0006 at N = 80 cycles. (a)The actual capacity regeneration points. (b) The detected capacity regeneration points.

B0007 and B0018 batteries are also carried out and the results is listed in Table 1. As shown in Table 1, almost all the detection accuracy are close to 100%. In terms of the recall rate, four batteries reach 100% except for B0018 at $N = 80$ cycles. At that time, the detection recall rate drops to 83.3%, which means only one capacity regeneration point is not detected.

4.2. The PF-AR model based RUL prediction results

As mentioned above, the PF-U algorithm is performed first to avoid the capacity regeneration points. Assume the prediction starting time (ST) is the ith cycle, the PF-U algorithm is used to detect the CRP by comparing the Mann-Whitney U test statistics at this point (the ith cycle) and the control limit. If the control limit is

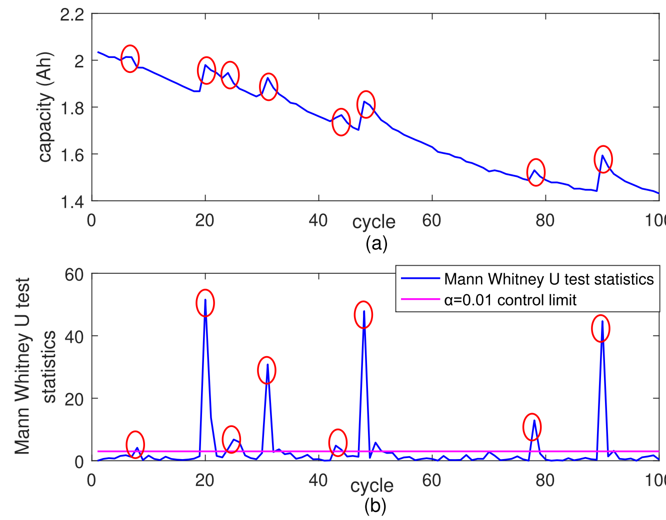

Fig. 6. The detection results of B0006 at N = 100 cycles. (a)The actual capacity regeneration points. (b) The detected capacity regeneration points.

Table 1
The detected capacity regeneration results of four batteries.

Dataset	Training cycles	Acc	Pre	RR
B0005	60	100%	100%	100%
	80	100%	100%	100%
	100	100%	100%	100%
B0006	60	96.67%	75%	100%
	80	97.5%	77.78%	100%
	100	98%	80%	100%
B0007	60	100%	100%	100%
	80	100%	100%	100%
	100	100%	100%	100%
B0018	60	98.33%	83.33%	100%
	80	97.5%	75%	83.3%
	100	98%	87.5%	100%

exceeded, $ST = i$ is replaced with $ST = i - 2$ to calculate $RUL_{ST=i} = RUL_{ST=i-2}$ by PF-AR algorithm. Otherwise, the $RUL_{ST=i}$ is predicted by the proposed PF-AR model directly.

The RUL prediction curve of lithium battery can be obtained when prediction ST is different. In order to show the influence of CRP detection on the RUL prediction accuracy, PF-AR model based RUL prediction with and without CRP detection are performed and compared in this subsection. Assume the prediction ST is gradually increase from the 80th cycle with the step size of 1. The prediction results of B0005 battery at different ST are shown in Fig. 7(a). From the figure, in the 90th cycle, the RUL error predicted by the PF-AR model based method without CRP detection is 29 cycles, while the error is only 2 cycles by the counterpart with CRP detection. The prediction accuracy at this point has been improved by 93% with CRP detection.

To prove the universality of the method, Fig. 7(b)–(d) and Table 2 shows the RUL prediction result of B0006, B0007 and B0018 batteries, respectively. It can be seen that the RUL prediction error has been greatly improved by PF-AR model based method with CRP detection. In addition, the $RMSE$ and R^2 of PF-AR model with CRP detection are superior to the counterpart without CRP detection. Especially for B0018 battery, the $RMSE$ and R^2 are improved by 71.8%

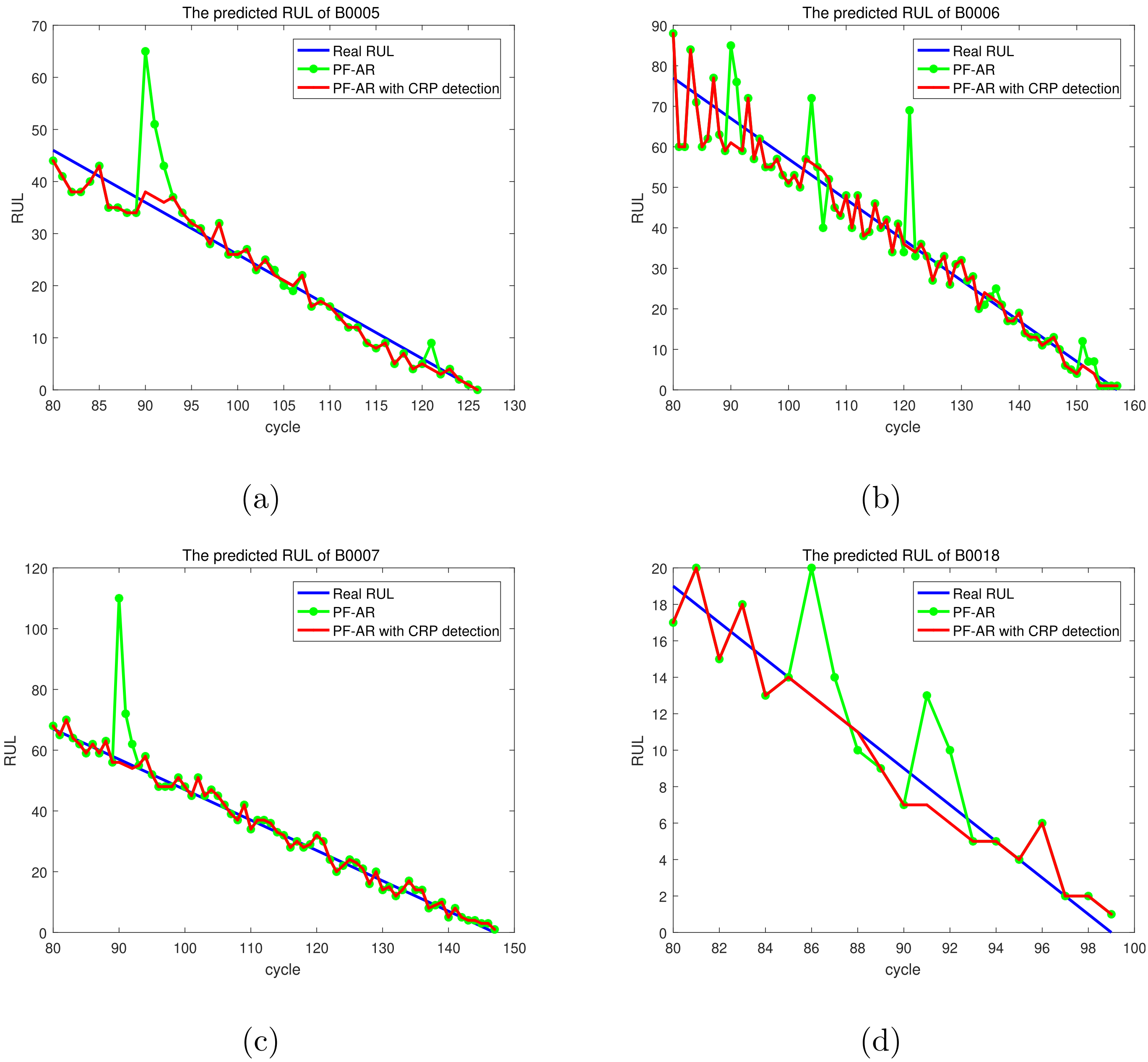

Fig. 7. The predicted RUL with and without CRP detection for B0005,B0006, B0007, and B0018.

Table 2
The influence of CRP detection on RUL prediction.

Methods	B0005		B0006		B0007		B0018	
	RMSE	R^2	*RMSE*	R^2	*RMSE*	R^2	*RMSE*	R^2
PF-AR	5.5887	0.8302	7.0292	0.9025	7.1630	0.8668	4.9447	0.2657
PF-AR with CRP detection	**2.4582**	**0.9672**	**4.8990**	**0.9527**	**2.3577**	**0.9856**	**1.3964**	**0.9414**
Improvement percentage	**56%**	**16.5%**	**30.3%**	**5.6%**	**67.1%**	**13.7%**	**71.8%**	**254.3%**

and 254.3% respectively.

On the other hand, in order to verify the superiority of the proposed RUL prediction method, it is compared with single PF, AR and SVR based methods. Fig. 8 shows the comparison results of B0005 battery by these four methods, and the RUL prediction result and the absolute error are shown in Fig. 8(a) and (b) respectively. It can be seen that the RUL predicted by the above four algorithms fluctuate with the real RUL curve, among which the proposed method has the smallest fluctuation range. The *RMSE* of the four method are 4.4002, 3.1724, 4.1540, 2.4582, and the R^2 are calculated as 0.8948, 0.9453, 0.9062, 0.9672 respectively. With the smallest *RMSE* and largest R^2, the proposed method has the superior

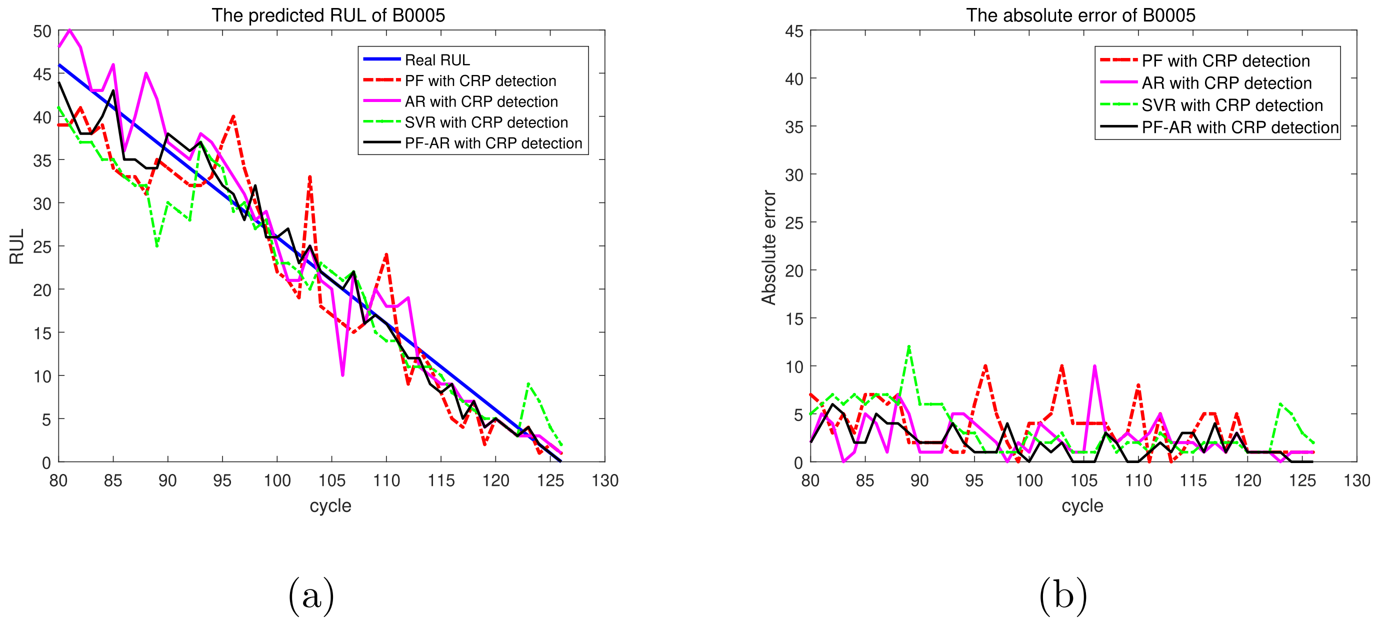

Fig. 8. RUL prediction results of four methods for B0005.

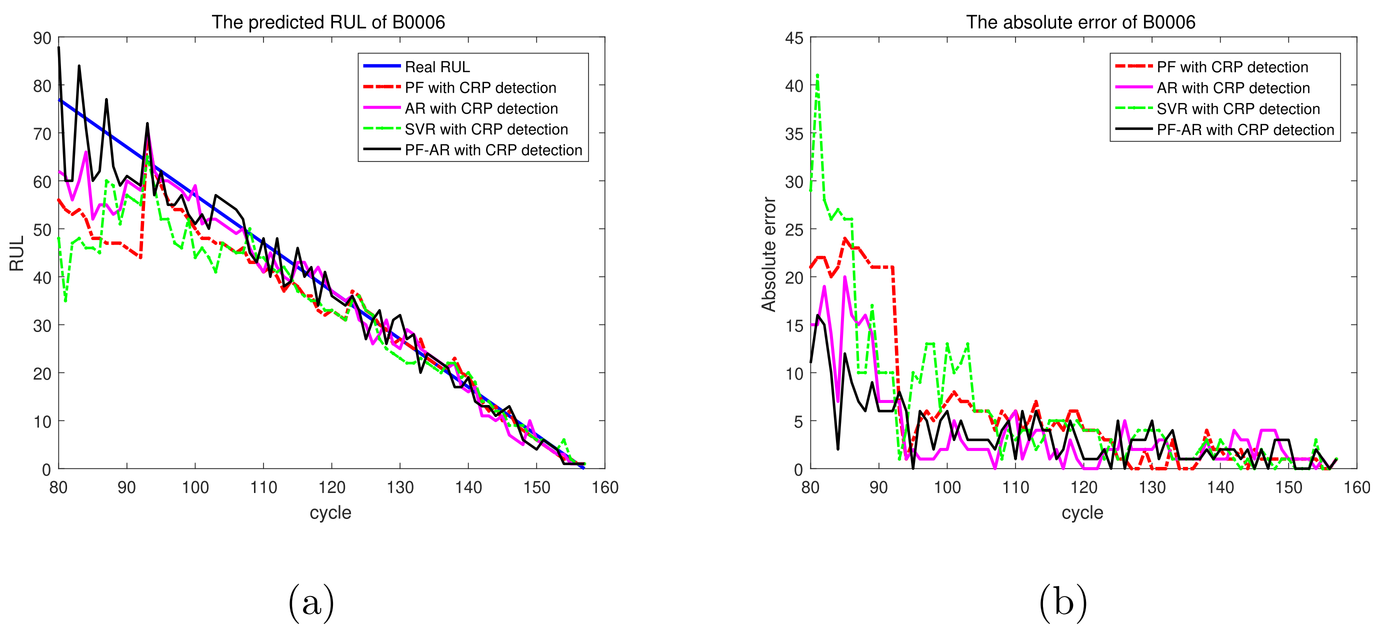

Fig. 9. RUL prediction results of four methods for B0006.

performance to PF, AR and SVR based methods.

Figs. 9–11 are the RUL prediction results and the corresponding absolute errors of B0006, B0007 and B0018 under the four aforementioned methods respectively. As can be seen from Figs. 10 and 11, the predicted RUL of B0007 and B0018 under the proposed method is the closest to actual RUL; meanwhile, the absolute error is closest to 0. For the battery B0006, although there is no obvious difference between the four methods in Fig. 9(a), the proposed method has the smallest error in 80–95 cycles according to Fig. 9(b).

In addition, the *RMSE* and R^2 of the four prediction models are listed in Table 3. It can be seen that among the above four batteries, *RMSE* of the proposed model is the smallest and its R^2 coefficient is the largest. Thus, the RUL prediction performance of the proposed method is superior to PF, AR and SVR based methods. Meanwhile, the improvement degree of the proposed method compared with the other methods in *RMSE* and R^2 indicators are quantified. From this table, the improvement of the proposed method compared to others is listed. For example, compared to PF method with CRP detection, the improvement of *RMSE* and R^2 are 71.7% and 20.2% in B0007 battery respectively.

Finally, we calculate the model mean response time (MRT) of the proposed method (PF-AR with CRP detection) and other methods. Take the B0007 battery as an example, the MRT of PF-AR, PF with CRP detection, AR with CRP detection, SVR with CRP detection and the proposed method are 7.94s, 16.43s, 10.12s, 10.67s, 17.7s respectively. The MRT of the proposed method is longer than others. The reason lies in that the CRP detection that is carried out

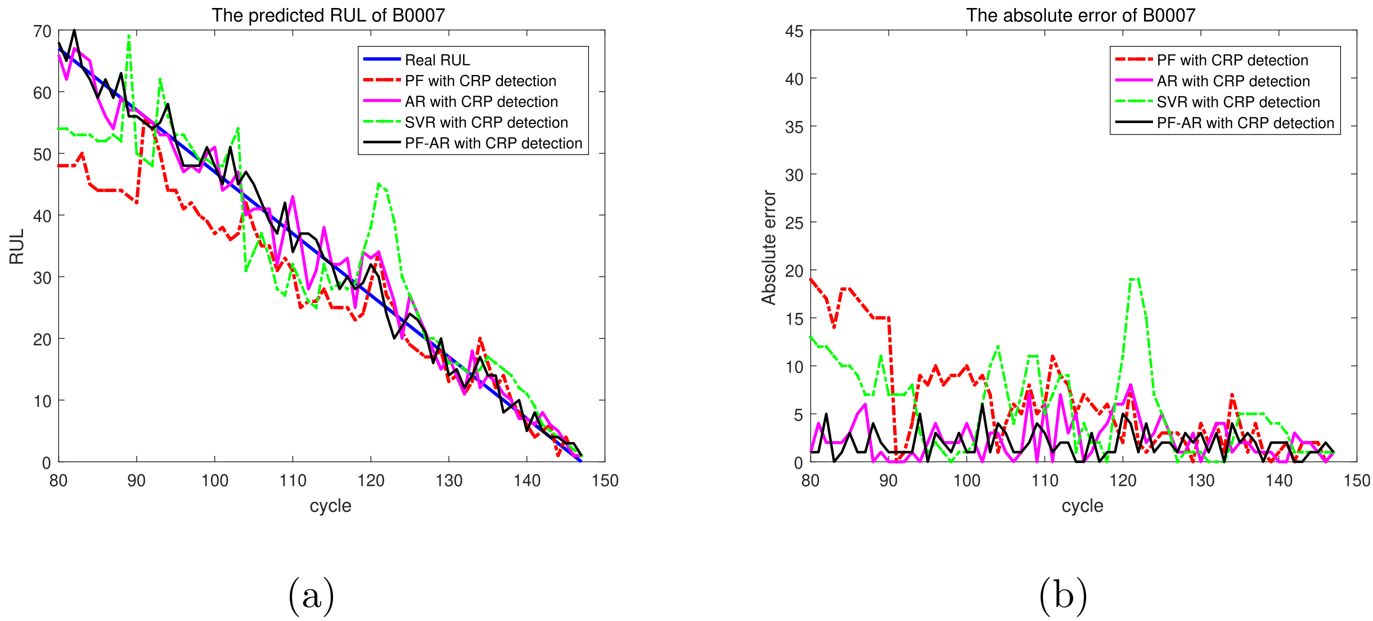

Fig. 10. RUL prediction results of four methods for B0007.

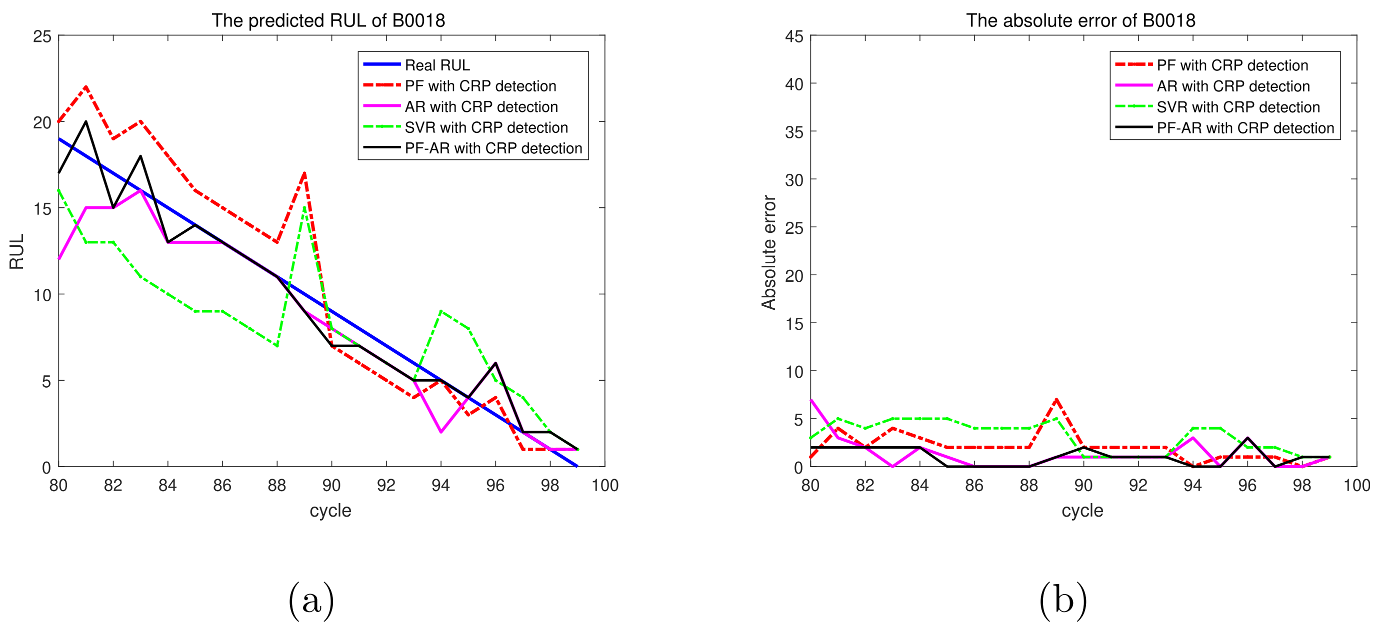

Fig. 11. RUL prediction results of four methods for B0018.

Table 3
The prediction performance and improvement of the proposed method compared with the other three methods.

Methods	B0005		B0006		B0007		B0018	
	RMSE	R^2	*RMSE*	R^2	*RMSE*	R^2	*RMSE*	R^2
PF with CRP detection	4.4002	0.8948	9.5360	0.8206	8.331	0.8198	2.5593	0.8030
Improvement percentage	**44.13%**	**8.1%**	**48.6%**	**16.1%**	**71.7%**	**20.2%**	**45.5%**	**17.2%**
AR with CRP detection	3.1724	0.9453	6.15920	0.9252	3.0989	0.9751	2.1331	0.8632
Improvement percentage	**22.51%**	**2.32%**	**20.5%**	**2.97%**	**23.9%**	**1.08%**	**34.5%**	**9.1%**
SVR with CRP detection	4.1540	0.9062	10.436	0.7852	7.2386	0.8640	3.4928	0.6331
Improvement percentage	**40.82%**	**6.73%**	**53.1%**	**21.3%**	**67.4%**	**14.1%**	**60%**	**48.7%**
PF-AR with CRP detection	**2.4582**	**0.9672**	**4.8990**	**0.9527**	**2.3577**	**0.9856**	**1.3964**	**0.9414**

first will cost some time. Although the MRT of our proposed method is the longest, it is only a few seconds longer than other models. And the order of magnitude for all the methods is the same, so it will not assert much negative influence on the cost of the batteries.

5. Conclusion

The existence of capacity regeneration of lithium battery makes the capacity degradation more complicated and will decrease RUL prediction accuracy. In order to eliminate the influence of CRP, this paper propose a PF-AR based RUL prediction method with PF-U based CRP detection for lithium battery. Firstly, by combining PF and Mann-Whitney *U* test theory, the battery capacity regeneration points are detected. Then, after replacing the CRPs with the points ahead of them, a method on basis of PF and AR model is presented for RUL prediction. Taking the predicted capacity of AR model as the 'actual' capacity, PF update the degradation model parameters to obtain the accurate RUL prediction. Finally, B0005, B0006, B0007 and B0018 batteries in the open dataset of NASA are adopted for the verification of the proposed method. Comparing with PF, AR and SVR based methods, the proposed method has superior performance in RUL prediction of the lithium battery.

However, for the PF-U based CRP detection method, although the CRPs are all detected, there are still some false positives. This will lead to a longer response time of the model. Therefore, how to eliminate false positives require further study in the future work.

Author statement

Qiuhui Ma: Conceptualization, Methodology, Software, Investigation, Data curation, Writing original draft, visualization. **Ying Zheng:** Conceptualization, Methodology, Formal analysis, Review and Editing, Supervision, Funding acquisition. **Weidong Yang:** Formal analysis, Review and Editing, Supervision. **Yong Zhang**: Review and Editing, Supervision, Funding acquisition. **Hong Zhang**: Review and Editing. **Jia-Lin Kang**: Conceptualization, Review and Editing, Resources.

Declaration of competing interest

The authors declare that they have no known competing financial interests or personal relationships that could have appeared to influence the work reported in this paper.

Acknowledgement

The work is supported by the National Natural Science Foundation of China (Grant 61873102 and 61873197), Key Natural Science Foundation of Hubei (Grant 2019CFA047), and MOE Key Laboratory of Image Processing and Intelligence Control (IPIC2018-10).

References

[1] Qu J, Liu F, Ma Y, Fan J. A neural-network-based method for RUL prediction and SOH monitoring of lithium-ion battery. IEEE Access 2019;7:87178–91.
[2] Swornowski P. Destruction mechanism of the internal structure in Lithium-ion batteries used in aviation industry. Energy 2017;122:779–86.
[3] Liu C, Wang Y, Chen Z. Degradation model and cycle life prediction for lithium-ion battery used in hybrid energy storage system. Energy 2019;166:796–806.
[4] Li Y, Wang W, Lin C, Yang X, Zuo F. A safety performance estimation model of lithium-ion batteries for electric vehicles under dynamic compression. Energy 2021;215:119050.
[5] Zheng C, Chen Z, Huang D. Fault diagnosis of voltage sensor and current sensor for lithium-ion battery pack using hybrid system modeling and unscented particle filter. Energy 2020;191:116504.
[6] Ma G, Zhang Y, Cheng C, Zhou B, Hu P, Yuan Y. Remaining useful life prediction of lithium-ion batteries based on false nearest neighbors and a hybrid neural network. Appl Energy 2019;253:113626.
[7] Wu L, Fu X, Guan Y. Review of the remaining useful life prognostics of vehicle lithium-ion batteries using data-driven methodologies. Appl Sci 2016;6(6):166.
[8] Liu D, Zhou J, Liao H, et al. A health indicator extraction and optimization framework for lithium-ion battery degradation modeling and prognostics. IEEE Transactions on Systems, Man, and Cybernetics: Systems 2015;45(6):915–28.
[9] Li X, Yuan C, Wang Z, Wang Y, et al. State-of-health estimation for Li-ion battery via partial incremental capacity analysis based on support vector regression. Energy 2020:117852.
[10] Deng Y, Ying H, Zhu H, et al. Feature parameter extraction and intelligent estimation of the State-of-Health of lithium-ion batteries. Energy 2019;176:91–102.
[11] Patil MA, Tagade P, Hariharan KS, et al. A novel multistage Support Vector Machine based approach for Li ion battery remaining useful life estimation. Appl Energy 2015;159:285–97.
[12] Pan H, Lv Z, Wang H, et al. Novel battery state-of-health online estimation method using multiple health indicators and an extreme learning machine. Energy 2018;160:466–77.
[13] Bian C, He H, Yang S. Stacked bidirectional long short-term memory networks for state-of-charge estimation of lithium-ion batteries. Energy 2020;191:116538.
[14] Safari M, Morcrette M, Teyssot A, Delacourt C. Multimodal physics-based aging model for life prediction of li-ion batteries. J Electrochem Soc 2009;156(3):A145–53.
[15] Tian J, Xu R, Wang Y, et al. Capacity attenuation mechanism modeling and health assessment of lithium-ion batteries. Energy 2021;221:119682.
[16] Yu J. State-of-Health monitoring and prediction of lithium-ion battery using probabilistic indication and state-space model. IEEE Transactions on Instrumentation and Measurement 2015;64(11):2937–49.
[17] Cadini F, Sbarufatti C, Cancelliere F, Giglio M. State-of-life prognosis and diagnosis of lithium-ion batteries by data-driven particle filters. Appl Energy 2019;235:661–72.
[18] Xiong R, Sun F. A data-driven multi-scale extended Kalman filtering based parameter and state estimation approach of lithium-ion polymer battery in electric vehicles. Appl Energy 2014;113:463–76.
[19] Pan H, Lv Z, Lin W, et al. State of charge estimation of lithium-ion batteries using a grey extended Kalman filter and a novel open-circuit voltage model. Energy 2017;138:764–75.
[20] He W, Williard N, Osterman M, Pecht M. Prognostics of lithium-ion batteries based on Dempster–Shafer theory and the Bayesian Monte Carlo method. J Power Sources 2011;196:10314–21.
[21] Shen D, Wu L, Kang G, et al. A novel online method for predicting the remaining useful life of lithium-ion batteries considering random variable discharge current. Energy 2021;218:119490.
[22] Xue Z, Zhang Y, Cheng C, et al. Remaining useful life prediction of lithium-ion batteries with adaptive unscented kalman filter and optimized support vector regression. Neurocomputing 2020;376:95–102.
[23] Zhang Y, Xiong R, He H, et al. Lithium-ion battery remaining useful life prediction with box–cox transformation and Monte Carlo simulation. IEEE Trans Ind Electron 2019;66:1585–97.
[24] Xing Y EWM, et al. An ensemble model for predicting the remaining useful life performance of lithium-ion batteries. Microelectron Reliab 2013;53(6):811–20.
[25] Pang X, Huang R, Wen J, et al. A lithium-ion battery RUL prediction method considering the capacity regeneration phenomenon. Energies 2019;12(12):1–14.
[26] Jin G, Matthews D, Zhou Z. A Bayesian framework for on-line degradation assessment and residual life prediction of secondary batteries in spacecraft. Reliab Eng Syst Saf 2013;113:7–20.
[27] Qin T, Zeng S, Guo J, et al. A rest time-based prognostic framework for state of health estimation of lithium-ion batteries with regeneration phenomena. Energies 2016;9(11):896.
[28] Deng L, Shen W, Wang H, Wang S. A rest-time-based prognostic model for remaining useful life prediction of lithium-ion battery. Neural computing and Applications 2020.
[29] Orchard ME, Lacalle MS, Olivares BE, et al. Information-theoretic measures and sequential Monte Carlo methods for detection of regeneration phenomena in the degradation of lithium-ion battery cells. IEEE Trans Reliab 2015;64(2):701–9.
[30] Wang D, Kong J, Zhao Y, Tsui Kwok-Leung. Piecewise model based intelligent prognostics for state of health prediction of rechargeable batteries with capacity regeneration phenomena. Measurement 2019.
[31] Saha B, Goebel K. Battery data set", NASA Ames prognostics data repository. Moffett Field, CA: NASA Ames Research Center; 2007. http://ti.arc.nasa.gov/project/prognostic-data-repository.
[32] Sanjeev Arulampalam M, Maskell Simon, Gordon Neil. A tutorial on particle filters for online nonlinear/non-Gaussian bayesian tracking. IEEE Trans Signal Process 2002;50(2):174–88.
[33] Ruxton GD. The unequal variance t-test is an underused alternative to Student's t-test and the Mann–Whitney U test. Behav Ecol 2006;17(4):688–90.